Sensitivity of on-line wavelength during retrieval of atmospheric CO_2 vertical profile

Wei Gong,[1,2] Ailin Liang,[1,*] Ge Han,[1] Xin Ma,[1] and Chengzhi Xiang[1]

[1]*State Key Laboratory of Information Engineering in Surveying, Mapping, and Remote Sensing, Wuhan University, 129 Luoyu Road, Wuhan 430079, China*

[2]*Collaborative Innovation Center of Geospatial Technology, 129 Luoyu Road, Wuhan 430079, China*

**Corresponding author: ireneliang@whu.edu.cn*

Received March 25, 2015; revised May 15, 2015; accepted May 15, 2015;
posted May 15, 2015 (Doc. ID 236724); published June 11, 2015

Accurately measuring the differential molecular absorption cross section is the key to obtaining a high-precision concentration of atmospheric trace gases in a differential absorption lidar (DIAL) system. However, the CO_2 absorption line is meticulous at 1.6 μm, easily translating and broadening because of the change of temperature and pressure. Hence, measuring the vertical profile of atmospheric temperature and pressure to calculate the vertical profile of the CO_2 weight parameter is necessary. In general, measuring atmospheric temperature and pressure has a certain amount of uncertainty. Therefore, this study proposes the concept of a balanced on-line wavelength, where the differential molecular absorption cross section is larger and the CO_2 weight parameter is insensitive to the uncertainty of atmospheric temperature and pressure. In this study, we analyzed the influence of uncertainty on the CO_2 weight parameter at every preselected wavelength, as well as determined an appropriate wavelength near one of the absorption peaks. Our result shows that 1572.023 nm should be one of the appropriate balanced on-line wavelengths. The measurement errors of the mixing ratio of CO_2 molecule in this wavelength are only 0.23% and 0.25% and are caused by 1 K temperature error and 1 hPa pressure error, respectively. This achievement of a balanced on-line wavelength will not only depress the requirement of the laser's frequency stabilization but also the demand for measurement precision of the atmospheric temperature and pressure profile. Furthermore, this study can achieve the exact measurement of the vertical profile of atmospheric CO_2 based on an independent differential absorption laser.

OCIS codes: (010.1290) Atmospheric optics; (280.3640) Lidar.
http://dx.doi.org/10.1364/PRJ.3.000146

1. INTRODUCTION

CO_2, a long-lived atmospheric trace species, is an important greenhouse gas [1–3], indicating the importance of detecting changes in atmospheric CO_2. Recently, several instruments of both passive and active remote sensing have been developed to map the global atmospheric CO_2 concentration at a large scale with high precision. Differential absorption lidar (DIAL) is currently a quite promising technique to detect atmospheric CO_2 concentration [4], especially in the lower atmosphere, which is close to human activities. DIAL has numerous advantages, such as nighttime coverage, availability of all latitudes, less interference by clouds and aerosol scattering, and precise column height determination [5–7]. Airborne or satellite-borne lidar measurements of atmospheric CO_2 using the integrated path differential absorption lidar (IPDA) technique, a special case of the DIAL technique, are promising approaches for retrieving global CO_2 column concentrations [8–10]. Active sensing of CO_2 emissions over nights, days, and seasons and advanced space carbon and climate observation of planet earth missions, aimed at global CO_2 column concentration measurement, had been proposed and researched by NASA and European Space Agency (ESA), respectively. Thus far, several sensitivity and simulation analyses on satellite-borne IPDA of CO_2 measurements exist [5,10,11], although such instruments are still under development. By contrast, an initiative for ground-based DIAL for CO_2 measurement has already been developed [12–15]. Ground-based DIAL systems are of great significance because they can provide atmospheric CO_2 measurements that are range-resolved, accurate, and have high temporal resolution to complement airborne and satellite-borne measurements. However, the developers of the DIAL system for DIAL CO_2 mixing ratio measurements are confronted with the very stringent requirements on measurement accuracy below 1% in CO_2 volume mixing ratio. DIAL CO_2 mixing ratio accuracy and precision depends on instrumental (for lidar CO_2 differential absorption measurement), spectroscopic, and meteorological data accuracies and precisions.

In the process of atmospheric CO_2 retrieval, the influence of temperature and pressure is not negligible. The overall influence of the temperature retrieval error on space-based measurement of atmospheric total column CO_2 is less than 0.05%, which is significantly smaller than the change; this result is attributed to the 1% CO_2 change in the planetary boundary layer [16]. However, the vertical CO_2 profile on ground-based DIAL is more sensitive to temperature [17]. Notably, a climatological temperature profile generally produces a relative error of 0.3–1.7 ppm/K in the space-borne estimate of the atmospheric CO_2 column [18]. The detection of the vertical profile of atmospheric CO_2 will produce a larger error because of the uncertainty of the atmospheric temperature profile. Similarly, the uncertainty of atmospheric pressure also has a certain influence on the CO_2 retrieving precision. Therefore, considering getting higher precision,

we suggest that the on-line wavelength should be fixed at the balanced on-line wavelength, but not at the absorption peak [12], if the atmospheric environment varies dramatically and the measurements of temperature or pressure profiles are inaccurate when the relevant wavelength control technique is available. Selection conditions of a balanced on-line wavelength include low temperature sensitivity, low pressure sensitivity, and low interference from other molecules.

Developing an independent instrument to observe the temporal range-resolved concentration of atmospheric CO_2 accurately is difficult because the biases caused by the uncertainty of temperature and pressure cannot be disregarded. Therefore, determining the balanced on-line wavelength can certainly improve the measurement accuracy of CO_2 concentration. This study analyzes the effect of temperature and pressure on retrievals and calculates the balanced on-line wavelength. The two major selected wavelengths for ground-based CO_2 DIAL sensing are ~1.57 and ~2.0 μm [13,14]. Based on the conclusion of Menzies [19], the wavelength range of 1.57 μm is not well suited for CO_2 retrievals in the lower troposphere, compared to 2.0 μm. However, the study of a 1.57 μm DIAL system has developed more rapidly than a 2 μm, which has some constraints [12]. Therefore, it is especially necessary to study the sensitivity of the on-line wavelength at 1.57 μm. As our system, a part of atmospheric profiling synthetic observation system (APSOS) [20], is designed to work at ~1.57 μm, the preselection of wavelength in this study is confined to ~1.57 μm. Moreover, we focus on the retrieving process of echo signal in the 1.57 μm band to the planetary boundary layer atmospheric CO_2 profile in relation to the response to a variable atmospheric environment. The presentation of the weight of temperature and pressure based on the retrieval presented in Section 2 is the innovation of this study. The influence of atmospheric temperature and pressure on the weight is the main factor for the measurement accuracy in the retrieving process of the DIAL system. Section 3 analyzes the effect of atmospheric temperature and pressure on weight and compares the retrieving error of different pre-selected on-line wavenumbers. Furthermore, the absorption cross selection is considered. Section 4 screens three segments of on-line wavelength that have lower sensitivity and larger absorption cross sections and discusses the results. Section 5 summarizes the most important findings of this study.

2. METHOD

The DIAL technique is a promising method for obtaining vertical profiles of atmospheric CO_2. This analysis method has an important role in the measurement of ozone, water vapor, CO_2, and other trace gases for over 30 years [10,21–24]. DIAL utilizes the absorption of detected molecules and scattering of atmosphere to obtain the damped echo signal. The efficiency of the absorption depends on the wavelength of the laser. A DIAL system transmits two laser beams of slightly different wavelengths, one at the on-line wavelength and one at the off-line wavelength, to eradicate the influence of other factors and obtain accurate information of the detected component. The lidar equation of backscatter signals at the on-line wavelength λ_{on} and off-line wavelength λ_{off} is as follows:

$$P_{on,off}(R) = \frac{P_0(\lambda_{on,off})\beta\eta A c\tau_p}{2R^2} * \exp\left(-2\int_0^R (N_W(z)\sigma_W(\lambda_{on,off}) + \alpha(\lambda_{on,off}, z))dz\right). \quad (1)$$

Here, P_{on} is the photon number on λ_{on} at range R, P_{off} is the photon number on λ_{off} at range R, P_0 is the transmitted photon number, β is the atmosphere backscatter coefficient, A is the telescope area, η is the overlap function, c is the speed of light, τ_p is the laser pulse width, $N_W(R)$ is the number density of detected molecules at range R, $\sigma_W(\lambda_{on,off})$ is the absorption cross section of detected molecules on λ_{on} or λ_{off}, and $\alpha(\lambda_{on,off}, R)$ is the atmospheric extinction coefficient at range R.

As the on-line wavelength and the off-line wavelength are very close, the atmosphere backscatter coefficient (β) at these two wavelengths are approximately the same, as well as the atmospheric extinction coefficient (α). When we analyze the signals from the same altitude, coefficient β and α can be viewed as the same. Thus, the number density of detected molecules at height R can be computed by

$$N_W(R) = \frac{1}{2(\sigma_W(\lambda_{on}) - \sigma_W(\lambda_{off}))\Delta R} * \ln\frac{P_{off}(R_{top})P_{on}(R_{bottom})}{P_{on}(R_{top})P_{off}(R_{bottom})}, \quad (2)$$

where R_{top} and R_{bottom} are the altitudes of the top and bottom of resolved range, respectively. The concentration of detected molecules is generally expressed by the volume proportion per atmospheric m^3. The conversion formula between number density and concentration can be described as follows:

$$C(R) = \frac{N_W(R)}{n} = \frac{N_W(R)rT}{A_v P}, \quad (3)$$

where A_v is 6.022×1023 mol^{-1} and r is 8.314 $J \cdot mol^{-1} \cdot K^{-1}$. Based on the formula, the process of the conversion is related to the atmospheric environment including temperature and pressure. However, previous studies of the DIAL detection of atmospheric CO_2 did not consider the influence of the measurement uncertainty of the atmospheric environment on the measurement accuracy. Thus, in the present study, we improved the algorithm of weight, which can be expressed as follows:

$$w = \frac{\sigma_W(\lambda_{on}) - \sigma_W(\lambda_{off})}{rT/A_v P}. \quad (4)$$

Therefore, the concentration function can be rewritten as

$$C(R) = \frac{1}{2w\Delta R} * \ln\frac{P_{off}(R_{top})P_{on}(R_{bottom})}{P_{on}(R_{top})P_{off}(R_{bottom})}. \quad (5)$$

This improvement has a great advantage in retrieving atmospheric CO_2 concentration and evaluating the precision of measurement. According to the function, the retrieving error of CO_2 concentration caused by the uncertainty of atmospheric temperature and pressure is absolutely determined by the weight function. As shown in Fig. 1, the relationship of these two kinds of error is nonlinear, which can be described as follows:

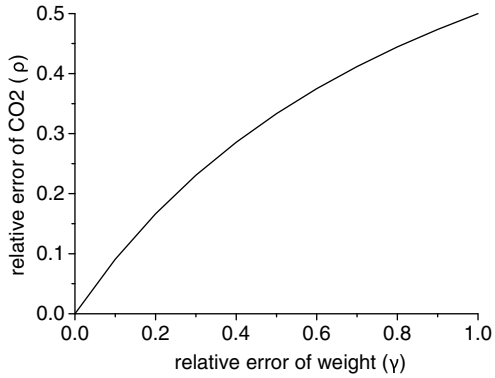

Fig. 1. Relationship of the relative error of CO_2 concentration (ρ) and that of weight (γ).

$$\rho = \frac{\Delta C}{C1} = \frac{|C2 - C1|}{C1} = \frac{|\frac{a}{w2} - \frac{a}{w1}|}{a/w1} = \frac{|w1 - w2|}{w2} = \frac{\Delta w}{\Delta w + w1} = \frac{\gamma}{\gamma + 1}, \tag{6}$$

where ρ is the relative error of CO_2 concentration, γ is the relative error of weight at the same wavelength, $\gamma = \frac{\Delta w}{w1}$ $(0 < \gamma < 1)$, $\Delta w = |w2 - w1|$, and $\Delta C = |C2 - C1|$. ρ and γ are the approximations of the full quadratic formulas.

According to Eq. (6), the calculation error of CO_2 concentration (ρ) will be less than 1% when the calculation error of weight (γ) is less than 1.11%. Thus, if the concentration of atmospheric CO_2 is 400 ppm, the error of weight must be controlled in approximately 1%, which can limit the error of CO_2 concentration down to 4 ppm.

Overall, the improvement of the accuracy of retrieval depends on the accuracy of weight. In the equation of a weighting function w, σ is also commonly given in pressure and temperature coordinates, which can be described as follows [25,26]:

$$\sigma_g(\nu) = \frac{yS(T)\sqrt{LN2}}{\gamma_D \pi^{3/2}} \int_{-\infty}^{+\infty} \frac{\exp(-t^2)}{(x - t)^2 + y^2} \mathrm{d}t, \tag{7}$$

where $y = \sqrt{\ln 2} * \gamma_L/\gamma_D$, $x = \sqrt{\ln 2} * (\nu - \nu_c)/\gamma_D$, ν_c is the central wavenumber, ν is the trial wavenumber, $S(T)$ is line intensity at temperature T, γ_L is Lorentzian half-width half-maximum (HWHM), varying with the given temperature T and pressure P, and γ_D is Doppler HWHM.

$$S(T) = S_0 \frac{T_0}{T} \exp\left(\frac{E'' \mathrm{hc}}{K_B}\left(\frac{1}{T_0} - \frac{1}{T}\right)\right), \tag{8}$$

$$\gamma_L = \gamma_0 \frac{P_0}{P}\left(\frac{T_0}{T}\right)^n, \tag{9}$$

$$\gamma_D = \frac{\nu_0}{c}\sqrt{\frac{2 \ln 2 * (k_B T)}{m}}, \tag{10}$$

$$\nu_c = \nu_0 + P/P_0 * (\delta_0(T_0) + \delta'(T - T_0)), \tag{11}$$

where P is the given pressure, P_0 and T_0 are the standard atmospheric pressure of 101325 Pa and temperature of 296.15 K, respectively, γ_0 is the reference line HWHM, n is the temperature dependence exponent of pressure-broadening coefficients, k_B is the Boltzmann constant, E is the lower energy state of the transition, h is Planck's constant, m is the molecular weight, ν_0 is the central wavenumber at 0 Pa and 296 K, δ_0 is the coefficient of pressure-induced shift, and δ' is the temperature dependence coefficient of δ_0.

The relative error of weight is absolutely determined by the measurement error of atmospheric temperature and pressure. In order to develop an independent instrument system, a DIAL system without any facilities used to measure the temperature and pressure profile, to detect the atmospheric CO_2 concentration, it is necessary to decrease the influence of the variation of atmospheric environment. Therefore, under the same uncertainty of atmospheric environment, decreasing the relative error of weight at the emitted wavelength as far as possible is the key to obtaining accurate results. The following section analyzes the sensitivity of temperature and pressure on retrieving weight of different wavenumbers.

3. ANALYSIS AND RESULT

Six absorption lines, including R10–R20, in the 30012 ← 00001 band of CO_2 are preselected because the intensities of these lines are evidently higher than those of the other lines. Most spectroscopic parameters of CO_2 lines are from Predoi-Cross *et al.* [27], who have the most updated data for CO_2 at the ~1.6 μm region. However, the lower energy level (E''), which governs the temperature sensitivity of the absorption cross section, is from HITRAN2012 [28]. According to a previous study, water vapor is considered the most significant interference molecule with respect to absorption spectroscopy [29]. Considering the effect of water vapor absorption, Fig. 2 shows that the third (R14), fourth (R16), and fifth (R18) regions of CO_2 are more appropriate for use as CO_2 DIAL, owing to the higher absorption cross section of CO_2 and the small effect of H_2O. Therefore, we discuss the effect on weight at the wavenumber range around these three regions, which is from 6358 to 6362 cm^{-1}.

Various approaches to obtaining the profile of the atmospheric temperature and pressure are available. The most common method is based on the 1976 U.S. Standard atmosphere model [30], which can be described by the following formulas: $T = 288.15 - 0.0065 * H$, $P = 1013.25 * (288.15/T)^{-5.25577}$. Here, $H \leq 11000$ m, which covers the detection range of atmospheric CO_2. However, the error of the profiles of atmospheric temperature and pressure is inevitable and could be 3 K/km and 4–10 hPa/km. Other methods that can obtain relatively higher precision can be acquired by microwave radiometers or balloon sounding data. Even though the precision can be improved by a degree, the errors of atmospheric temperature and pressure still reach 1 K/km and 1 hPa/km, respectively. Thus, an appropriate balanced on-line wavelength should be used in an independent DIAL system to reduce the effect of the error on the weight as far as possible. This section then analyzes the effect on different on-line wavelengths in two parts, namely, temperature and pressure.

A. Sensitivity of Temperature on the Weight

When the pressure is constantly set to 1013.25 hPa, regardless of the on-line wavelength, the trend of the weight decreasing with increasing temperature from 256 to 296 K is similar, as

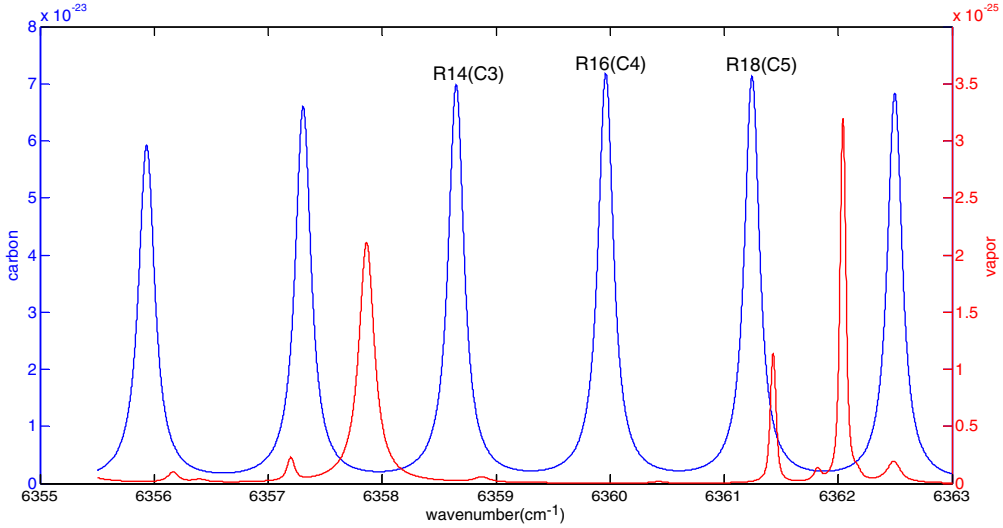

Fig. 2. Absorption cross section of CO_2 and H_2O with respect to wavenumber near ~1.57 μm. The blue line sharing the left vertical axis depicts the absorption cross section of CO_2. The red line that marks the right axis depicts the absorption cross section of H_2O.

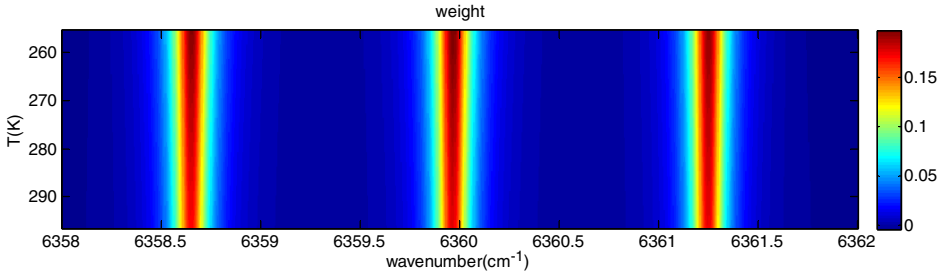

Fig. 3. Weight in continuous temperature at three wave bands. The colorful area sharing the right color bar depicts the weight of different wavenumbers (horizontal axis) on continuous temperature (left axis).

shown in Fig. 3. The only difference is the gradient of decrease, which represents the sensitivity of temperature. When the measurement error of temperature is 1 K, the relative error of the retrieval is the relative variation of weight. The relative error of weight [γ(T)] at different wave bands varies, as shown in the scatter curves in Fig. 4. The calculation is an average of a 40 K uncertainty of atmospheric temperature range up and down at the center of the current temperature. It shows that the relative error of weight [γ(T)] is less than 0.9% on most wavenumbers, and the R14 seems to be more sensitive to the change of temperature than the other two wave bands. Besides, the most insensitive points of three wave bands slightly left deviate from the absorption peaks, and the degree of deviation gets bigger as the wavenumber of absorption peak gets bigger. When the wavenumber is far away from the most insensitive points, the relative error increases rapidly until the off-line wavenumber. Considering the influence of the uncertainty of the atmospheric temperature, to determine the insensitive balanced on-line wavelength, the average of the relative error should be smaller than 0.33% because the measurement error of the atmospheric temperature is more or less 3 K. Additionally the absorption cross section of the balanced on-line wavelength should be enough larger than the off-line wavelength that it fulfills the consideration that the optic depth of atmospheric CO_2 can ensure a better signal-to-noise ratio (SNR) for the system. On screening the preselected wavenumbers, the appropriate on-line wavenumbers are notably 6368.625–6358.655 cm^{-1} near the 6359.654 (R14) peak, 6359.940–6359.975 cm^{-1} near the 6359.967 (R16) peak, and 6361.220–6361.265 cm^{-1} near the 6361.250 (R18) peak, the absorption cross section $\sigma_W(\lambda_{on})$ of which is larger than 90% of the corresponding absorption peak.

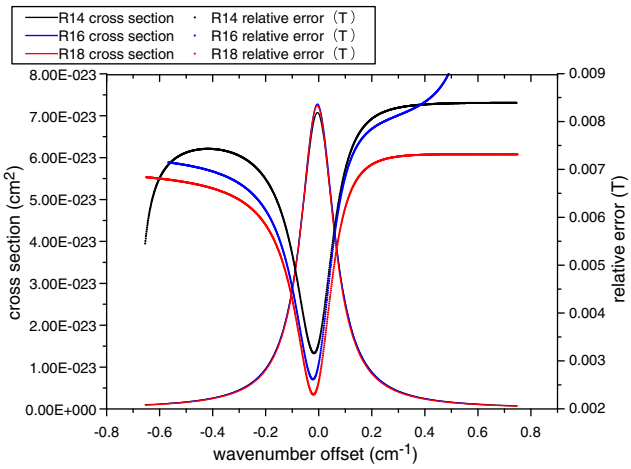

Fig. 4. Relative error of weight [γ(T)] and cross section at three wave bands. The lines sharing the left axis depict the absorption cross section and the scatter curves sharing the right axis depict the relative error of weight when there is the uncertainty of atmospheric temperature. Three colors represent three wave bands, black corresponding to R14, blue corresponding to R16, and red corresponding to R18.

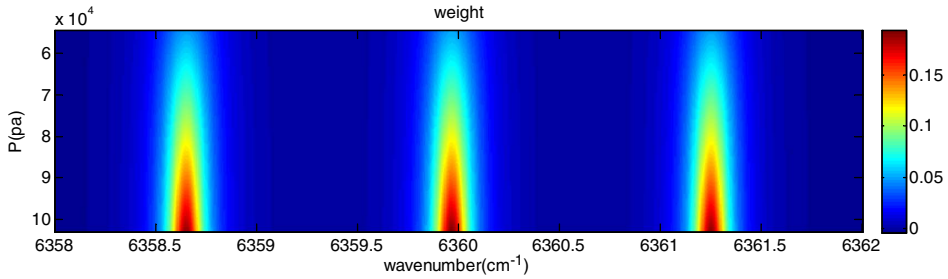

Fig. 5. Weight in continuous pressure on multiple on-line wavenumber. The colorful area sharing the right color bar depicts the weight of different wavenumbers (horizontal axis) on continuous pressure (left axis).

B. Sensitivity of Pressure on the Weight

Both the temperature and pressure vary at the detection range in a vertical measurement. The measurement of atmospheric pressure is more accurate than that of the temperature at the same range. Thus, 1 hPa is an appropriate range span to calculate the weight in the pressure profile. In this simulation, the temperature was set to 288.15 K, which is the surface temperature according to the 1976 U.S. standard atmospheric model. With the pressure continuously increasing, the weight increases, as shown in Fig. 5. Similar to the analysis of the sensitivity of temperature on the weight, Fig. 6 shows that the relative error of weight [γ(P)] is less than 3% at most wavenumbers. It illustrates that the influence of the uncertainty of atmospheric pressure is smaller than that of atmospheric temperature on the retrieval. Similarly, the relative error of weight at the R18 wave band seems to be less than the others. But the trends of the relative weight [γ(P)] variations are absolutely contrary to γ(T).The most insensitive point of pressure is hardly any deviation from the absorption peak at any wave bands, and the relative error decreases rapidly when the wavelength is far from the peaks until the off-line wavelength. Considering the influence of the uncertainty of atmospheric pressure, to determine the insensitive balanced on-line wavelength, the average of the relative error should be smaller than 0.33%, which is already satisfied.

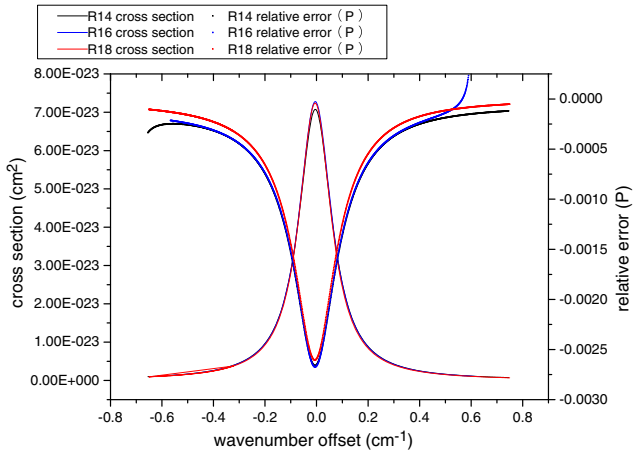

Fig. 6. Relative error of weight [γ(P)] and cross section at three wave bands. The lines sharing the left axis depict the absorption cross section and the scatter curves sharing the right axis depict the relative error of weight when there is uncertainty of atmospheric pressure. Three colors represent three wave bands, black corresponding to R14, blue corresponding to R16, and red corresponding to R18.

C. Sensitivity on Differential Molecular Absorption Cross Section

Based on the analysis of the former two parts, the influence of the uncertainty of atmospheric temperature on the weight is more than that of pressure at three wave bands as a whole. But the two kinds of relative error of weight are more or less at wavenumbers close to the absorption peaks. Compared to the others, the R18 wave band has less sensitivity to the uncertainty of atmospheric temperature and pressure. Moreover, another important consideration is the differential molecular absorption cross section. It is necessary that the differential molecular absorption cross section should be always enough larger at the detection range to ensure available retrieval. Taking the 1976 U.S. Standard atmosphere model as the average atmospheric temperature and pressure, Fig. 7 shows the differential molecular absorption cross section of three wave bands as the atmosphere environment changes at the detection range. The differential molecular absorption cross section at the wavenumbers close to absorption peaks in any altitude is more than the other wavenumbers, although it decreases as the altitude increases. Another point for consideration is that the variation near the absorption peak is fiercer than the others. In general, when the altitude is higher than 3 km, the difference around the absorption peak is less than 5e-23 cm^2, and the accuracy of results will be slightly lower. However, the error is unavoidable. Additionally, selecting a wavelength close to the absorption peak as the on-line wavelength has another advantage: It is beneficial for frequency stabilization [31,32]. Thus, an on-line wavelength fulfilling the consideration is top priority to be selected to obtain a perfect signal and retrieve a high accuracy result.

To satisfy the three previously stated requirements—namely, reducing the effects of temperature and of pressure and keeping a large differential molecular absorption cross section at the detection range—we screen for the wavenumbers from 6358 to 6362 cm^{-1} and determine the balanced on-line wavelength. Figure 8 displays the sequence of appropriate wavenumbers of three wave bands, where the absorption cross section is more than 90% of that at their respective absorption peak, with the lower sensitivity of atmospheric temperature and pressure. The average of the absorption cross section of the wavenumbers at the R16 wave band is slightly larger than that of the others, whereas the sensitivity of the temperature and pressure at the R18 wave band is the lowest. Therefore, we suggest the balanced on-line wavelength should be selected at the most insensitive wavelength of R18 wave band. However, the comprehensive extinction coefficient notably gets larger, when there are thick clouds or hazes. The

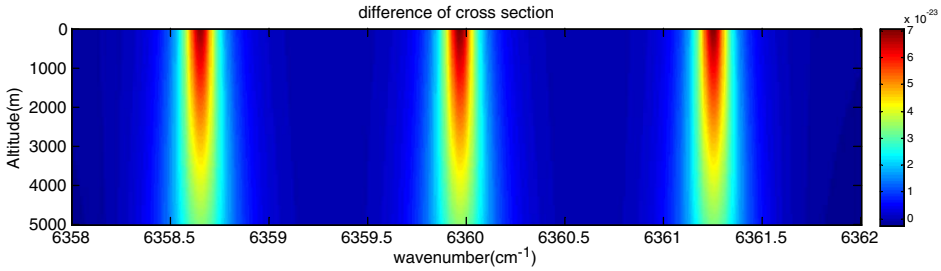

Fig. 7. Differential molecular absorption cross section at the range of 5 km at three wave bands. The colorful area sharing the right color bar (in cm^2) depicts the value of differential molecular absorption cross section at three wave bands (horizontal axis in cm^{-1}) at continuous altitude (left axis in m).

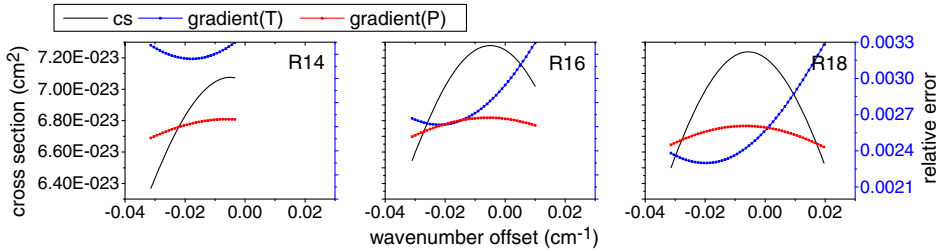

Fig. 8. Sensitivity of atmospheric temperature and pressure on the relative error of weight with the absorption cross section at the range of wavenumbers near each absorption peak of three wave bands, R14, R16, and R18. The three figures have the same scale of vertical axes. Black curves depict the absorption cross section, sharing the left axis in cm^2. Blue curves depict the relative error of weight as the temperature varies according to the analysis in Section 3.A. Red curves depict the relative error of weight as the pressure varies according to the analysis in Section 3.B. Blue and red curves share the right axis.

signal we receive will be weaker, which is not beneficial for retrieval. In order to get a good signal to noise ratio, it is advisable to strengthen the contrast of on-line and off-line echo signal. Regardless of the chosen option, a 3 K error of temperature and a 3 hPa error of pressure are allowable at the sequence of appropriate wavelengths. In other words, the wavenumbers shown in Fig. 8 are good choices to be the on-line wavenumbers to have less error in the retrieval. Among those regions, 1572.023 nm should be the most appropriate balanced on-line wavelengths, where the measurement of errors of the mixing ratio of the CO_2 molecule is only 0.23% and 0.25% caused by 1 K temperature error and 1 hPa pressure error, respectively. The balanced on-line wavelength we suggest has a 0.02 cm^{-1} left offset from the R18 absorption peak. And the R18 absorption peak has similar sensitivity to the least sensitivity in the R16 CO_2 absorption line, which has 0.02 cm^{-1} left offset from the center.

4. CONCLUSION

This study presents an improvement to retrieve more accurate vertical profiles of CO_2 concentration by decreasing the effects of both temperature and pressure uncertainty. The comprehensive influence of atmospheric temperature and pressure on retrieving the vertical profile of CO_2 concentration was evaluated in this study for the first time. The key difference with previous studies is considering two processes in retrieval. One is the shift of the absorption cross section because of the variation of atmospheric temperature and pressure. The other is the conversion from the initial result in $mol \cdot m^{-3}$ to a concentration in ppm. Most studies ignored the second influence. We improved the weight function, taking the two sources of influence into consideration. Therefore, the error of weight determines the error of retrieval caused by the atmospheric temperature and pressure. Furthermore, we proposed a concept of balanced on-line wavelength that considered the absorption cross of CO_2 molecule, as well as the error resulting from the uncertainty of atmospheric temperature and pressure. The analysis on the improved weight function plays an important role in calculating the balanced on-line wavelength, which should be applied in an independent DIAL system. Meanwhile, a clear understanding of the effect of atmospheric temperature and pressure on the weight will contribute to the accuracy of the evaluation of the retrievals. Based on the analysis, we suggest the balanced on-line wavelength should be 1572.023 nm in the R18 CO_2 absorption line. However, continuous research on stabilizing the on-line wavelength at ~1.57 μm of pulsed laser systems must be performed.

ACKNOWLEDGMENTS

This work was supported by the National Natural Science Foundation of China (Grant No. 41127901) and the Program for Innovative Research Team in University of Ministry of Education of China (Grant No. IRT1278).

REFERENCES

1. C. Field and M. Van Aalst, *Climate Change 2014: Impacts, Adaptation, and Vulnerability* (IPCC, 2014).
2. J. E. Bauer, W. J. Cai, P. A. Raymond, T. S. Bianchi, C. S. Hopkinson, and P. A. Regnier, "The changing carbon cycle of the coastal ocean," Nature **504**, 61–70 (2013).
3. I. Y. Fung, S. C. Doney, K. Lindsay, and J. John, "Evolution of carbon sinks in a changing climate," Proc. Natl. Acad. Sci. USA **102**, 11201–11206 (2005).
4. D. Bruneau, F. Gibert, P. H. Flamant, and J. Pelon, "Complementary study of differential absorption lidar optimization in direct and heterodyne detections," Appl. Opt. **45**, 4898–4908 (2006).

5. G. R. Allan, H. Riris, J. B. Abshire, X. Sun, E. Wilson, J. F. Burris, and M. A. Krainak, "Laser sounder for active remote sensing measurements of CO_2 concentrations," in *Aerospace Conference* (IEEE, 2008), pp. 1–7.
6. S. Houweling, W. Hartmann, I. Aben, H. Schrijver, J. Skidmore, G.-J. Roelofs, and F.-M. Breon, "Evidence of systematic errors in SCIAMACHY-observed CO_2 due to aerosols," Atmos. Chem. Phys. **5**, 3003–3013 (2005).
7. R. J. Engelen and G. L. Stephens, "Information content of infrared satellite sounding measurements with respect to CO_2," J. Appl. Meteorol. **43**, 373–378 (2004).
8. S. Kameyama, M. Imaki, Y. Hirano, S. Ueno, S. Kawakami, D. Sakaizawa, and M. Nakajima, "Performance improvement and analysis of a 1.6 μm continuous-wave modulation laser absorption spectrometer system for CO_2 sensing," Appl. Opt. **50**, 1560–1569 (2011).
9. J. B. Abshire, H. Riris, G. R. Allan, C. J. Weaver, J. P. Mao, X. L. Sun, W. E. Hasselbrack, S. R. Kawa, and S. Biraud, "Pulsed airborne lidar measurements of atmospheric CO_2 column absorption," Tellus B **62**, 770–783 (2010).
10. G. Ehret, C. Kiemle, M. Wirth, A. Amediek, A. Fix, and S. Houweling, "Space-borne remote sensing of CO_2, CH_4, and N_2O by integrated path differential absorption lidar: a sensitivity analysis," Appl. Phys. B **90**, 593–608 (2008).
11. S. Kawa, J. Mao, J. Abshire, G. Collatz, X. Sun, and C. Weaver, "Simulation studies for a space-based CO_2 lidar mission," Tellus B **62**, 759–769 (2010).
12. G. J. Koch, J. Y. Beyon, F. Gibert, B. W. Barnes, S. Ismail, M. Petros, P. J. Petzar, J. Yu, E. A. Modlin, and K. J. Davis, "Side-line tunable laser transmitter for differential absorption lidar measurements of CO_2: design and application to atmospheric measurements," Appl. Opt. **47**, 944–956 (2008).
13. F. Gibert, P. H. Flamant, J. Cuesta, and D. Bruneau, "Vertical 2-μm heterodyne differential absorption lidar measurements of mean CO_2 mixing ratio in the troposphere," J. Atmos. Ocean. Technol. **25**, 1477–1497 (2008).
14. D. Sakaizawa, S. Kawakami, M. Nakajima, Y. Sawa, and H. Matsueda, "Ground-based demonstration of a CO_2 remote sensor using a 1.57 μm differential laser absorption spectrometer with direct detection," J. Appl. Remote Sens. **4**, 043548 (2010).
15. L. Fiorani, S. Santoro, S. Parracino, M. Nuvoli, C. Minopoli, and A. Aiuppa, "Volcanic CO_2 detection with a DFM/OPA-based lidar," Opt. Lett. **40**, 1034–1036 (2015).
16. J. Mao and S. R. Kawa, "Sensitivity studies for space-based measurement of atmospheric total column carbon dioxide by reflected sunlight," Appl. Opt. **43**, 914–927 (2004).
17. G. Han, W. Gong, H. Lin, X. Ma, and Z. Xiang, "Study on influences of atmospheric factors on vertical co_2 profile retrieving from ground-based DIAL at 1.6 μm," IEEE Transactions on Geoscience Electronics **53**, 3221–3234 (2015).
18. E. Dufour and F.-M. Bréon, "Spaceborne estimate of atmospheric CO_2 column by use of the differential absorption method: error analysis," Appl. Opt. **42**, 3595–3609 (2003).
19. R. T. Menzies and D. M. Tratt, "Differential laser absorption spectrometry for global profiling of tropospheric carbon dioxide: selection of optimum sounding frequencies for high-precision measurements," Appl. Opt. **42**, 6569–6577 (2003).
20. D. Lu and W. Pan, "Atmospheric profiling synthetic observation system (APSOS)," AIP Conf. Proc. **1531**, 244–247 (2013).
21. E. Browell, S. Ismail, and W. Grant, "Differential absorption lidar (DIAL) measurements from air and space," Appl. Phys. B **67**, 399–410 (1998).
22. U. Platt and D. Perner, "Direct measurements of atmospheric CH_2O, HNO_2, O_3, NO_2, and SO_2 by differential optical absorption in the near UV," J. Geophys. Res. **85**, 7453–7458 (1980).
23. K. Ikuta, N. Yoshikane, N. Vasa, Y. Oki, M. Maeda, M. Uchiumi, Y. Tsumura, J. Nakagawa, and N. Kawada, "Differential absorption lidar at 1.67 μm for remote sensing of methane leakage," Jpn. J. Appl. Phys. **38**, 110 (1999).
24. P. F. Ambrico, A. Amodeo, P. Di Girolamo, and N. Spinelli, "Sensitivity analysis of differential absorption lidar measurements in the mid-infrared region," Appl. Opt. **39**, 6847–6865 (2000).
25. B. Armstrong, "Spectrum line profiles: the Voigt unction," J. Quant. Spectrosc. Radiat. Transfer **7**, 61–88 (1967).
26. E. V. Browell, S. Ismail, and B. E. Grossmann, "Temperature sensitivity of differential absorption lidar measurements of water vapor in the 720-nm region," Appl. Opt. **30**, 1517–1524 (1991).
27. A. Predoi-Cross, A. McKellar, D. C. Benner, V. M. Devi, R. Gamache, C. Miller, R. Toth, and L. Brown, "Temperature dependences for air-broadened Lorentz half-width and pressure shift coefficients in the 30013 ← 00001 and 30012← 00001 bands of CO_2 near 1600 nm," Can. J. Phys. **87**, 517–535 (2009).
28. L. Rothman, I. Gordon, Y. Babikov, A. Barbe, D. Chris Benner, P. Bernath, M. Birk, L. Bizzocchi, V. Boudon, and L. Brown, "The HITRAN2012 molecular spectroscopic database," J. Quant. Spectrosc. Radiat. Transfer **130**, 4–50 (2013).
29. A. Amediek, A. Fix, M. Wirth, and G. Ehret, "Development of an OPO system at 1.57 μm for integrated path DIAL measurement of atmospheric carbon dioxide," Appl. Phys. B **92**, 295–302 (2008).
30. A. J. Krueger and R. A. Minzner, "A mid-latitude ozone model for the 1976 US Standard Atmosphere," J. Geophys. Res. **81**, 4477–4481 (1976).
31. K. Numata, J. R. Chen, S. T. Wu, J. B. Abshire, and M. A. Krainak, "Frequency stabilization of distributed-feedback laser diodes at 1572 nm for lidar measurements of atmospheric carbon dioxide," Appl. Opt. **50**, 1047–1056 (2011).
32. G. Wertheim, M. Butler, K. West, and D. Buchanan, "Determination of the Gaussian and Lorentzian content of experimental line shapes," Rev. Sci. Instrum. **45**, 1369–1371 (1974).